STEM CELLS AND DEVELOPMENT
Volume 23, Number 13, 2014

DOI: 10.1089/scd.2014.0014

Patient-Derived Skeletal Dysplasia Induced Pluripotent Stem Cells Display Abnormal Chondrogenic Marker Expression and Regulation by *BMP2* and *TGFβ1*

Biagio Saitta,[1–3] Jenna Passarini,[1,2] Dhruv Sareen,[1,3] Loren Ornelas,[3] Anais Sahabian,[3] Shilpa Argade,[1,2] Deborah Krakow,[4,5] Daniel H. Cohn,[5,6] Clive N. Svendsen,[1,3] and David L. Rimoin[1,2,*]

Skeletal dysplasias (SDs) are caused by abnormal chondrogenesis during cartilage growth plate differentiation. To study early stages of aberrant cartilage formation in vitro, we generated the first induced pluripotent stem cells (iPSCs) from fibroblasts of an SD patient with a lethal form of metatropic dysplasia, caused by a dominant mutation (I604M) in the calcium channel gene *TRPV4*. When micromasses were grown in chondrogenic differentiation conditions and compared with control iPSCs, mutant *TRPV4*-iPSCs showed significantly ($P < 0.05$) decreased expression by quantitative real-time polymerase chain reaction of *COL2A1* (IIA and IIB forms), *SOX9*, *Aggrecan*, *COL10A1*, and *RUNX2*, all of which are cartilage growth plate markers. We found that stimulation with *BMP2*, but not *TGFβ1*, up-regulated *COL2A1* (IIA and IIB) and *SOX9* gene expression, only in control iPSCs. *COL2A1* (Collagen II) expression data were confirmed at the protein level by western blot and immunofluorescence microscopy. *TRPV4*-iPSCs showed only focal areas of Alcian blue stain for proteoglycans, while in control iPSCs the stain was seen throughout the micromass sample. Similar staining patterns were found in neonatal cartilage from control and patient samples. We also found that *COL1A1* (Collagen I), a marker of osteogenic differentiation, was significantly ($P < 0.05$) up-regulated at the mRNA level in *TRPV4*-iPSCs when compared with the control, and confirmed at the protein level. Collagen I expression in the *TRPV4* model also may correlate with abnormal staining patterns seen in patient tissues. This study demonstrates that an iPSC model can recapitulate normal chondrogenesis and that mutant *TRPV4*-iPSCs reflect molecular evidence of aberrant chondrogenic developmental processes, which could be used to design therapeutic approaches for disorders of cartilage.

Introduction

Skeletal dysplasias (SDs) are a heterogeneous group of more than 450 disorders that are associated with skeletal deformity, dwarfism, craniofacial malformations, joint degeneration, perinatal lethality, and other medical issues [1]. The incidence of these disorders is collectively almost 1:5,000 live births. Medical and surgical treatments are attempted to improve the quality of life of affected individuals with only limited results. These defects result from the disruption of normal chondrogenesis, the earliest phase of skeletal development, which occurs when mesenchymal cells commit to the chondrocyte lineage for cartilage growth plate development [2]. Many of the genes, their biochemical properties, and pathways have been defined [1].

The *TRPV4* gene encodes the transient receptor potential vanilloid family member 4, calcium channel protein. Heterozygous mutations in this gene result in a spectrum of dominantly inherited SD phenotypes [3–8]. *TRPV4* is a tetrameric calcium-permeable ion channel that plays a role in chondrocyte differentiation [9–13]. The first molecular defect in *TRPV4* was described for brachyolmia, a relatively mild condition characterized by short stature, a short trunk, and scoliosis [3]. Next, other distinct mutations were found in *TRPV4* for the moderate severity spondylometaphyseal dysplasia Kozlowski type (SMDK) and the nonlethal and

[1]Department of Biomedical Sciences, Cedars-Sinai Medical Center, Los Angeles, California.
[2]Medical Genetics Institute, Cedars-Sinai Medical Center, Los Angeles, California.
[3]Regenerative Medicine Institute of Cedars-Sinai Medical Center, Los Angeles, California.
[4]Departments of Human Genetics, Obstetrics & Gynecology, University of California Los Angeles, Los Angeles, California.
[5]Department of Orthopaedic Surgery and Orthopaedic Hospital Research Center, University of California Los Angeles, Los Angeles, California.
[6]Department of Molecular, Cell, and Developmental Biology, University of California Los Angeles, Los Angeles, California.
*Deceased.

lethal forms of metatropic dysplasia [4,5]. The perinatal lethal form of metatropic dysplasia has an extremely severe phenotype, including severe shortening of the long bones and a small chest with perinatal death resulting from cardiopulmonary compromise [5]. The majority of the *TRPV4* mutations seen in SDs are single amino-acid substitutions. In vitro electrophysiological studies have shown that these mutations activate the calcium channel with an increased basal activity [3–5,12]. This leads to the loss of normal ion pore gating and increased intracellular calcium levels [11,12], consistent with a gain-of-function mechanism. However, reduced channel activity was reported for *TRPV4* mutations in the mild disorder, familial digital arthropathy-brachydactyly (*FDAB*), which is primarily characterized by osteoarthropathy in the hands [7]. *TRPV4* mutations, sometimes in the same region of the gene, can show highly variable phenotypes that affect the skeleton, the peripheral nervous system, or both [6,8,13]. Several mechanisms for such phenotypes have been suggested, including: defects in Ca^{2+} homeostasis in chondrocytes or in motor and sensory neurons, abnormal protein-protein interactions, or dysregulation of gene expression during chondrocyte differentiation [13]. The mechanism by which *TRPV4* mutation causes SD is unclear, and a major limitation of current cellular models is that they cannot replicate the range of *TRPV4* activity during chondrogenesis, as they are transfection models which result in overexpressed homotetrameric mutant channels [3–5,7,12].

Historically, induced pluripotent stem cells (iPSCs) were first established from mouse fibroblasts using defined factors [14] and subsequently from human adult fibroblasts [15,16]. The iPSC technology that replicates human disease in the culture dish [17] has already been used to model phenotypes of several disorders [18], including ALS [19,20], muscular dystrophy, Huntington's disease [21], Parkinson's disease [22], spinal muscular atrophy [23], Marfan syndrome [24], and osteogenesis imperfecta [25]. Recently, using an in vitro cartilage defect model system, it has been shown that differentiated mouse iPSCs can be used for functional cartilage repair [26]. In addition, using different in vitro techniques, it has been reported that human embryonic stem (ES) cells [27,28] and human iPSCs [29–31] could be directed toward chondrogenic differentiation. We focused on the development of a human in vitro iPSC model of chondrogenesis to identify molecular pathways that might be altered in a neonatal lethal form of metatropic dysplasia. This approach utilizes the natural heterozygous state of the mutation in each iPSC line to understand the impact of specific mutations on signaling during chondrogenic differentiation.

Here, we report for the first time that patient-derived iPSCs can recapitulate dysregulated processes of cartilage development and that markers of cartilage growth plate formation, including the transcription factor *SOX9* [32,33], type II collagen [34–36] *Aggrecan*, and type X collagen [37,38], were significantly down-regulated over time in patient *TRPV4*-iPSCs when compared with the control. In addition, both bone morphogenetic protein 2 (*BMP2*) and transforming growth factor beta 1 (*TGFβ1*), two key regulators of chondrogenesis [39,40], cartilage repair [41] and used to obtain direct chondrogenic differentiation of human ES cells in vitro [28], showed abnormal signaling in patient iPSCs. This is the first indication that developmental processes, beyond activation of the calcium channel, could underlie this lethal form of metatropic dysplasia and provide proof-of-concept evidence that in vitro iPSC models can be used to dissect molecular mechanisms in cartilage disorders, an important first step toward potential treatment.

Materials and Methods

SD TRPV4-*iPSC generation using nonintegrating episomal vectors*

Human neonatal skin fibroblasts were obtained from the International Skeletal Dysplasia Registry (ISDR) of Cedars-Sinai Medical Center. Fibroblasts from a patient (R08-023) with lethal metatropic dysplasia, caused by a mutation (I604M) in the calcium gene *TRPV4*, were reprogrammed by the iPSC core (www.cedars-sinai.edu/RMI) to generate integration-free iPSCs under the guidelines of the Stem Cell Research Oversight Committee at Cedars-Sinai. Briefly, 8×10^5 fibroblasts were cultured [42] and nucleofected using Nucleofector II (Amaxa) and episomal plasmid expression vectors pCXLE-hUL, pCXLE-hSK, and pCXLE-hOCT3/4-shp53-F (Addgene) as reported [43]. Of the 20 isolated clones, three independent *TRPV4*-iPSC clones (23i-n1F, 23i-n12F, and 23i-n14F) were further expanded in mTeSR1 (Stemcell Technologies), characterized for pluripotency, and used for differentiation experiments. Control iPSC lines 83i-n1 and 14i-n6, used for all the assays, were previously described [44].

Sequencing of TRPV4-*iPSC clones*

Heterozygous mutation of *TRPV4* was confirmed in the iPSC clones. Briefly, bidirectional sequence analysis was performed as described [5], and the resulting sequences were compared with the reference for *TRPV4*, with nucleotide numbering starting from the A of the ATG initiation codon. The I604M substitution, in case R08-023, occurs in the cytoplasmic loop between the TM4 and TM5 domains [5].

Immunofluorescence of pluripotent markers

As reported [44], iPSCs grown on coverslips coated with Matrigel (BD Biosciences) were incubated with antibodies for *OCT4*, *SSEA-4*, and *SOX2* (Millipore) and with Alexa-Fluor-conjugated secondary antibodies AF488 and/or AF594 (Molecular Probes). Nuclei were counterstained with Hoechst 33258. Images were captured using a fluorescence microscope (Olympus BX51).

Embryoid-body formation and reverse transcription polymerase chain reaction

To determine germ layer formation capacity, iPSCs were plated in poly-HEMA coated flasks with embryoid-body (EB) media [20]. Spontaneous EB differentiation was assayed at 0, 14, and 28 days. Total RNA was extracted from EBs, according to the manufacturer's protocol (Qiagen), and 1 μg was reverse transcribed into cDNA, using a High-Capacity Reverse Transcription kit (Applied Biosystems). Reverse transcription polymerase chain reaction (RT-PCR) reactions were carried out using 400 nM of specific forward and reverse primers (Supplementary Table S1; Supplementary Data are available online at www.liebertpub.com/scd); 2× MyTaq HS PCR Mix (Bioline) and 10 ng per reaction of each cDNA was

used. RT-PCR was run with the MJ Research PTC-200 (Peltier Thermal Cycler) and carried out in 25 μL final volumes using the following conditions: 95°C 1 min (1 cycle), 95°C 15 s, 58°C 15 s, 72°C 10 s, (35 cycles), and 72°C 1 min (1 cycle). EB PCR products of markers expressed from all three germ-layers included ectoderm: *MSX1*, *PAX6*; mesoderm: *HAND1*, *BMP4*; endoderm: *AFP*, *GATA4*, and *SOX17*; pluripotent marker *TDGF1* [45]; and housekeeping control *GAPDH* were assayed and run on 1.5% Agarose (Sigma-Aldirich) gels, containing Ethidium bromide (Sigma) with a 100 bp ladder (BioLabs).

Alkaline phosphatase staining

Alkaline phosphatase (AP) staining was done using the Alkaline Phosphate II staining kit (StemGent) according to the manufacturer's protocol with positive staining showing pink/purple for AP.

Karyotyping

It was performed at Cedars-Sinai by the Cytogenetics Lab. Ten high-resolution G-banded metaphase cells from each iPSC clone were assessed for chromosomal rearrangements, using standard techniques [46].

Chondrogenic differentiation of iPSC micromasses on matrigel

Chondrogenic differentiation of pluripotent stem cells was induced under serum-free conditions using a modified version of a protocol previously described [47]. The iPSCs were grown on Matrigel (BD Biosciences) as a micromass (200,000 cells/each) using chondrogenic media (CM) with *BMP2* (CMB) or *TGFβ1* (CMT), (Peprotech). Normal fibroblast-derived iPSC lines 83i-n1 and 14i-n6 were obtained from the iPSC Core at Cedars-Sinai. iPSCs were cultured to confluency in mTeSR1 media, trypsinized using TryPLE Express (Life Technologies) for 5 min at 37°C, spun for 1 min at room temperature (RT), washed in 1× phosphate buffered saline (PBS), and resuspended in mTeSR1 to obtain a single cell suspension. A 24-well plate (Fisher Scientific) for each iPSC line and/or clone was used by coating the center of each well with 10 μL Matrigel for 1 h at RT. Cells were replated at a density of 2×10^5 cells as a ''micromass'' using 10 μL of mTeSR1 per well. After 2 h at 37°C in a humidified 5% CO2, 0.4 mL of the same medium was slowly added to each well. After 24 h, the media was replaced, only in samples used for chondrogenic differentiation, with Dulbecco's modified Eagle's medium (DMEM) high glucose containing 10% fetal bovine serum, 10% knockout serum replacement (KSR) and 1% Pen/Strep (Life Technologies). At day 1, the cultures were supplied with CM consisting of DMEM high glucose with sodium pyruvate and L-glutamine and containing 1% KSR, 1% Pen/Strep, 1% MEM Non-essential Amino Acids, 1% ITSX (Life Technologies), 10 μg/mL BSA, 50 μg/mL Ascorbic acid, 40 μg/mL L-Proline, and 10^{-7} M Dexamethasone (Sigma), or CM supplemented with either 100 ng/mL of recombinant human *BMP2* (CMB) or 10 ng/mL of recombinant human *TGFβ1* (CMT). Media (mTSeR1, CM, CMB, or CMT) was changed every 3 days throughout the treatment. Total RNA, protein, and micromass sections (described next) were prepared, and the media was also collected at 7, 14, and 21 days.

Alcian blue and Alizarin red staining

Micromass wells and cartilage tissue sections were fixed in 4% Paraformaldehyde, washed with 1× PBS, and incubated for 1 h with 0.5% Alcian Blue (Sigma) in 3% glacial acetic acid (pH 1.0). After incubation, the samples were washed with 3% glacial acetic acid (pH 1.0) once, followed by 3% glacial acetic acid (pH2.5) twice. Cartilage tissue sections were incubated for 1 h with 0.5% Alizarin red S (Sigma) at pH 4.2 and washed twice with distilled water. All samples were allowed to dry before imaging. Stained samples were imaged with a digital inverted microscope, EVOS xl core (AMG-Life Technologies).

PluriTest: bioinformatics based assay for pluripotency

A gene-chip and bioinformatics assay, PluriTest [48], using Illumina HT12 arrays, representing 23,000 genes, was utilized to determine *TRPV4*-iPSC clone pluripotency. The array was run at the UCLA genomics core (www.semel.ucla.edu/ungc), while the iPSC core at Cedars-Sinai performed data analysis.

Quantitative real-time polymerase chain reaction

Total RNA and cDNA were prepared as described earlier. All quantitative real-time polymerase chain reaction (qPCR) reactions were performed in triplicate in 10 μL reactions containing 10 ng cDNA, 400 nM forward and reverse primers, and 2× POWER SYBR Mix (Applied Biosystems). Reactions were run on a Viia7 System (Applied Biosystems) with the following parameters: 95°C for 8 min, followed by 40 cycles of 95°C for 15 s, 60°C for 1 min, and 72°C for 5 min. Results were analyzed using the $2^{-\Delta\Delta Ct}$ method, with *GAPDH* as the endogenous control and iPSCs (control or SD) at day 0 as the reference sample set to a value of 1. Statistical analysis was performed using an unpaired Student *t*-test and chi square test. A probability (*P*) value ≤ 0.05 was considered statistically significant.

Western blot analysis for type I (COL1) and type II (COL2) collagens

Conditioned Media (1 mL) was collected from micromass differentiation experiments at specific time points. Media was concentrated to 10× using Amicon Ultra 20K centrifuge spin columns according to the manufacturer's protocol (Millipore). Samples were loaded and run on a 4%–12% Tris-glycine stacking gel (Novex) with SDS buffer using the XCell SureLock Mini cell unit (Life Technologies). The blots were transferred, blocked in 5% milk, and incubated with COL2 monoclonal Ab3092 (Abcam) or with COL1 polyclonal 600-401 (Rockland) antibodies. Bands were visualized using an ECL Plus kit (Thermo Fisher Scientific).

Immunofluorescence of cartilage and bone markers

Micromasses were fixed in 4% PFA, followed by 30% sucrose, removed from tissue culture plates, frozen in OCT, sectioned in 10 μm sections using a cryostat 1850 (Leica), and incubated with polyclonal antibodies for COL2 (*COL2A1*) Ab300 (Abcam) or COL1, 600-401 (Rockland).

Results

Generation and characterization of iPSCs from an SD patient with a neonatal lethal form of metatropic dysplasia and mutation in TRPV4

To study abnormal cartilage formation in vitro, we utilized cells from an SD patient with a mutation (I604M) in *TRPV4*. The mutation results in perinatal lethal disease caused by the disruption of normal cartilaginous growth plate development [5]. To develop an in vitro model of chondrogenesis, we reprogrammed skin fibroblasts from the patient carrying the lethal *TRPV4* mutation, using six factors (*OCT3/4, SOX2, KL4, L-MYC, LIN28*, and *P53 shRNA*) in three episomal plasmids [43]. We then generated integration-free SD *TRPV4*-iPSC lines derived from the patient's cells and three clones (23i: n1F, n12F, and n14F) were selected and characterized for pluripotency (Fig. 1). Figure 1A

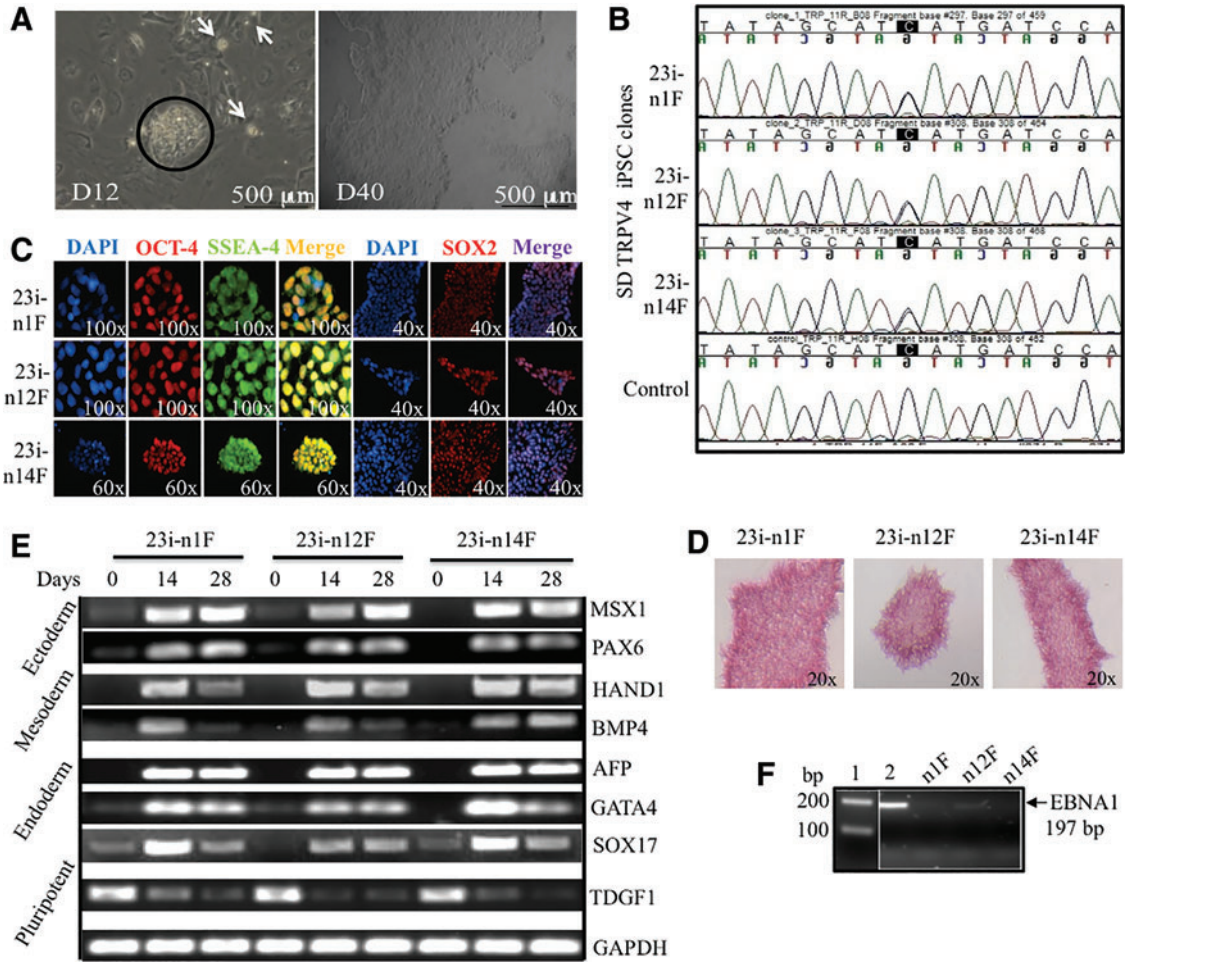

FIG. 1. Generation and pluripotency characterization of three independent *TRPV4*-iPSC clones isolated from nucleofected fibroblasts of a skeletal dysplasia (SD) patient with neonatal lethal metatropic dysplasia. **(A)** Phase-contrast images of nucleofected SD fibroblasts at day 12 in culture (D12) show the formation of several small iPSC colonies (*white arrows*) with large colony circled (*left*); day 40 (D40) shows the characteristic morphology of an iPSC colony after the first passages. The scale bar size is 500 µm. **(B)** DNA sequencing analysis of three iPSC clones (23i-n1F, 23i-n12F, and 23i-n14F) confirms the heterozygous mutation in exon 11 C1812>G (I604M) of the calcium channel gene *TRPV4*. Control human DNA sequence for *TRPV4* is shown for comparison (*bottom*). **(C)** Immunofluorescence staining of the three *TRPV4*-iPSC clones for pluripotent markers**:** *OCT4*, *SSEA4* (n1F and n12F, 100×; n14F, 60×), and *SOX2* (n1F-n14F, 40×), were used to confirm their pluripotency and counterstained with DAPI to show nuclei. **(D)** Alkaline phosphatase (AP) staining of the three 23i iPSC clones where the *pink/purple staining* indicates AP activity characterizing undifferentiated iPSCs. **(E)** RT-PCR of genes representing all three germ layers during embryoid body formation in vitro. All three 23i *TRPV4*-iPSC clones were tested at 0, 14, and 28 days for the expression of *MSX1* and *PAX6* (Ectoderm), *HAND1*, *BMP4* (Mesoderm), *AFP*, *GATA4*, *SOX17* (Endoderm), *TDGF1* as a pluripotent marker, and *GAPDH* as a housekeeping control. RT-PCR products were separated on a 1.5% agarose gel. Specific primers and band sizes obtained are listed in Supplementary Table S1. **(F)** Genomic PCR of the episomal plasmid gene Epstein-Barr nuclear antigen 1 (*EBNA1*) using DNA isolated from the three *TRPV4* iPSC clones at early passages (P10-P15). PCR products were separated on a 1.5% agarose gel and confirmed absence (23i-n1F, 23i-n14F) or near absence (23i-n12F) of the episomal vector compared with a positive control (lane 2) showing a band of 197 bp. DNA size ladder (100 bp) is shown in lane 1. iPSC, induced pluripotent stem cell; RT-PCR, reverse transcription polymerase chain reaction. Color images available online at www.liebertpub.com/scd

displays the formation of several iPSC colonies (white spots) seen at day 12 in culture where a larger colony is circled. The phase-contrast image taken at day 40 in culture shows the characteristic morphology of a typical human iPSC colony after its initial passages: a homogenous, flat appearance with well-defined edges [15,16]. Figure 1B presents a DNA sequence analysis of the three iPSC clones where both a C and a G peak are seen on standard sequencing, confirming that the heterozygous mutation in exon 11 of *TRPV4*, C1812>G (I604M) [5] is present in all of the patient 23i *TRPV4*-iPSC clones used for further experiments. Control human DNA sequence for *TRPV4* is shown for a comparison in the bottom panel. Figure 1C, pluripotency is confirmed by evaluating the expression of the *OCT4*, *SSEA4*, and *SOX2* markers using specific immunofluorescence staining. In Figure 1D, we show that all three 23i *TRPV4*-iPSC clones stained positive for AP, consistent with undifferentiated iPSCs [20]. EB formation was also assessed in vitro and Figure 1E displays the expression of genes from all three germ layers: Ectoderm (*MSX1* and *PAX6*), Mesoderm (*HAND1*, *BMP4*), and Endoderm (*AFP*, *GATA4*, and *SOX17*). *TDGF* was used as a marker of pluripotency [45], and *GAPDH* was used as a housekeeping control for these experiments. Figure 1F confirms absence of the episomal vector [43] in the newly generated 23i *TRPV4* clones using a genomic PCR assay for the Epstein-Barr nuclear antigen 1 (*EBNA1*) gene (Supplementary Table S1). A faint band seen in the n12F clone in these early passage iPSCs did not appear in later passages (after passage 20). The primers utilized for expression, integration analysis, and their band sizes are presented in Supplementary Table S1. Genomic stability was assessed by karyotyping and was normal for all three clones. A normal karyotype for one representative clone (23i-n14F) is shown (Supplementary Fig. S1). To further confirm the pluripotency of the iPSC clones, we next tested gene expression profiles using a recently developed PluriTest assay [48]. As shown in Table 1 and in Supplementary Fig. S2, all three 23i *TRPV4* clones passed the PluriTest, with a Pluripotency raw score >20 and Novelty score thresholds <1.6, and were therefore employed for all of the differentiation experiments performed in these studies.

The potential and limitations of the PluriTest, and its comparison with the teratoma assay to determine whether a specific iPSC line is pluripotent, have been discussed in depth [48]. Overall, these data demonstrate successful reprogramming of three independent 23i *TRPV4*-iPSC clones derived from skin fibroblasts of an SD patient with lethal metatropic dysplasia. Using standard assays for pluripotency [20] and a bioinformatics based-assay, PluriTest [48], we determined the expression of appropriate pluripotent markers and that the disease-causing mutation was present in every characterized 23i *TRPV4*-iPSC clone (Fig. 1).

Direct differentiation of control and SD TRPV4-*iPSCs micromasses into chondrogenic lineages*

Next, to establish an in vitro method for direct differentiation of iPSCs into lineages that can recapitulate progression of chondrogenesis [38], we used the distinct 23i *TRPV4*-mutant clones and the control iPSC lines 83i-n1 and 14i-n6 generated from reprogrammed control human fibroblasts and previously described [20]. For chondrogenic differentiation, control and SD *TRPV4*-iPSC lines were grown on Matrigel as micromass cultures in either iPSC medium (mTeSR; mT) [49], CM [47] or CM supplemented with 100 ng/mL of *BMP2*; (CMB) or with 10 ng/mL of *TGFβ1*; (CMT) [28], for 7, 14, or 21 days before whole mount staining with Alcian blue. This vital dye stains sulfated proteoglycans, which are characteristic of developing cartilage, as first described in micromass cultures of chondroprogenitor cells [50]. It has been used to determine accumulation over time of proteoglycan-rich matrix in human ES cells [28], in human iPSCs, and in iPSC-derived mesenchymal stem cells [31], all of which are grown as micromasses. Figure 2A and B shows micromasses stained with Alcian blue, where the accumulation of proteoglycans over time was evidenced by positive staining of iPSC micromasses grown in CM, with *BMP2* (CMB) or *TGFβ1* (CMT), but not in iPSC media (mT), demonstrating that chondrogenic differentiation can be reproduced in this model system. However, when comparing control versus *TRPV4* mutant iPSC lines at 14 and 21 days (grown in CM, CMB, or CMT), we found that while Alcian blue staining in controls (Fig. 2A) was seen throughout the sample, the mutant showed focal areas of stain (Fig. 2B). These differences were clearer in CM and CMB conditions where a more intense staining was observed compared with the CMT condition.

To compare our in vitro chondrogenic model with actual human cartilage tissue, we used the biobank resources of the ISDR, curated for decades by the late Dr. Rimoin and colleagues, to compare the micromass iPSC model with samples of neonatal cartilage taken from the patient whose fibroblasts were used for generating the *TRPV4*-iPSCs. Figure 2C shows normal neonatal cartilage, while Figure. 2D shows the patient's neonatal cartilage sections stained with Alizarin red for developing bone [51] or Alcian blue for cartilage [50]. In control sections, Alizarin red staining was uniform and localized to the periphery of the invading ossification margin (Fig. 2C, left panel). This staining was abnormal in the *TRPV4* patient's tissue and was not limited to the peripheral ossification area (Fig. 2D, left panel), but ''islands'' of positive staining were seen within the cartilage, suggesting altered chondrocyte differentiation in the growth plate, as reported for this disorder [5]. Overall, *TRPV4* patient cartilage shows irregular Alcian blue and

Table 1. PluriTest Score of Three Independent 23i *TRPV*4-Mutant-Induced Pluripotent Stem Cell Clones

23i TRPV4-iPSC clones	*Pluri raw*	*Pluri logit P*	*Novelty*	*Novelty logit P*	*PluriTest results*
23i-n1F	27.575	1	1.294	0.003	Pass
23i-n12F	21.354	1	1.509	0.027	Pass
23i-n14F	29.934	1	1.232	0.002	Pass

iPSC, induced pluripotent stem cell.

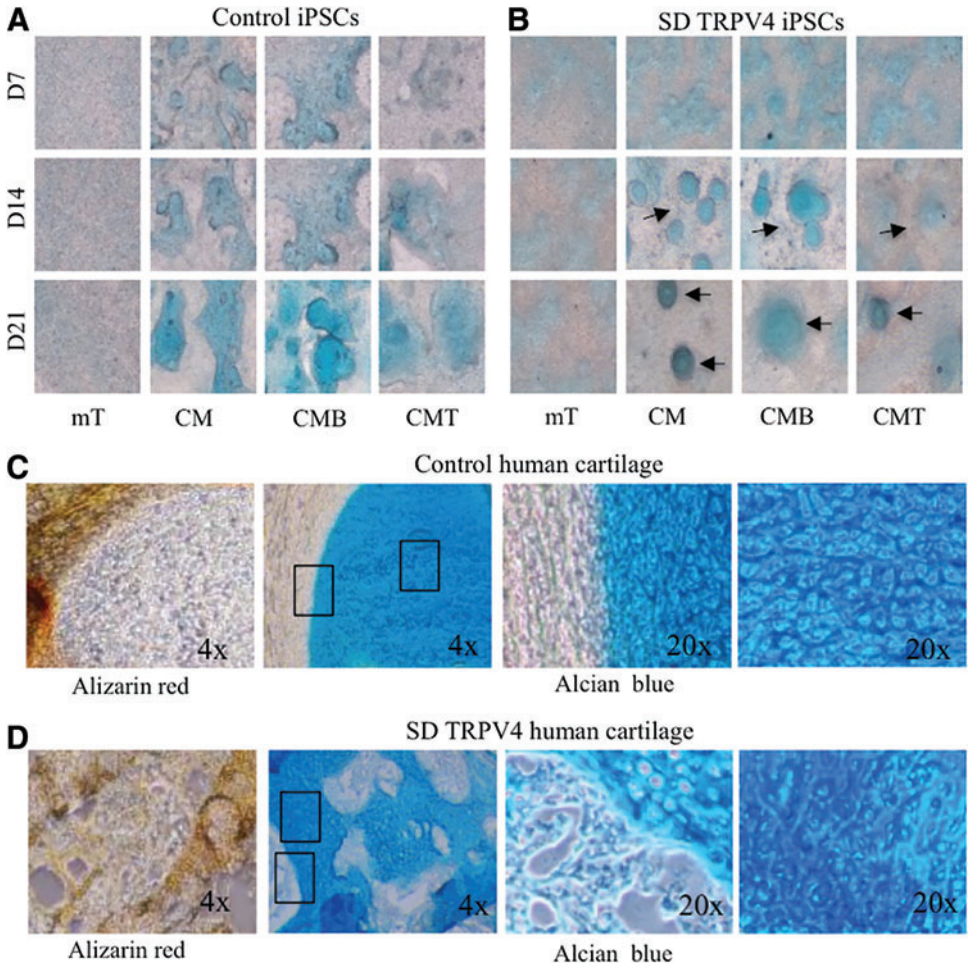

FIG. 2. Alcian blue and Alizarin red tissue-specific staining of control and *TRPV4*-iPSC micromass cultures and neonatal cartilage from control human and *TRPV4* patient samples. **(A, B)** Phase-contrast microscopy images (4×) of iPSC lines grown in micromass culture and stained with Alcian blue for sulfated proteoglycans of cartilage. Micromasses were grown in control iPSC medium (mTeSR; mT), chondrogenic medium (CM), or in CM supplemented with 100 ng/mL of *BMP2* (CMB) or with 10 ng/mL of *TGFβ1* (CMT) for 7, 14, or 21 days before whole mount staining. One representative clone for each control (83i-n1) and SD *TRPV4* mutant (23i-n14) iPSC line is shown. Focal stains are indicated by *arrows* **(B)**. Experiments were repeated at least thrice, using the control (14i-n6) and SD *TRPV4* mutant (23i-n12). **(C, D)** Phase-contrast images of control neonatal human cartilage sections **(C)** and SD *TRPV4* patient cartilage **(D)** stained with Alizarin red for developing bone or Alcian blue for cartilage. *Boxed outline areas* shown at 20× in adjacent photos **(C, D)**. *BMP2*, bone morphogenetic protein 2; *TGFβ1*, transforming growth factor beta 1. Color images available online at www.liebertpub.com/scd

Alizarin red staining compared with the control cartilage. This finding corroborates the staining seen for the control and *TRPV4*-iPSC lines, where Alcian blue staining from control and *TRPV4* lines show differences in morphology.

Impaired up-regulation of cartilage growth plate markers (SOX9, COL2A1, Aggrecan, COL10A1, and RUNX2), in TRPV4*-iPSCs during chondrogenic differentiation in vitro*

Type II collagen (COL2) is the characteristic and most abundant fibrillar collagen of cartilage, synthesized as a procollagen homotrimeric $[(\alpha 1)II]_3$ structural protein, which consists of a triple-helical domain flanked by N-and C-propeptides [34]. During fibril assembly, the propeptides are removed by specific proteases to generate the native COL2 molecules [52]. Its gene, *COL2A1*, encodes two main alternatively spliced procollagen forms defined by the inclusion (IIA) or exclusion (IIB) of exon 2 of 207 bp [35]. Expression of these procollagen isoforms is developmentally regulated and chondroprogenitor cells express mainly IIA, while differentiated chondrocytes express predominantly IIB [53]. To confirm that early stages of chondrogenesis were represented in our iPSC chondrogenic model, we used qPCR to examine the expression of the IIA and IIB spliced forms of COL2. We found that *COL2A1*, form IIA (Fig. 3A), and form IIB (Fig. 3B) significantly ($P < 0.05$) increased over time at 7, 14, and 21 days in culture in both controls and *TRPV4*-iPSCs. However the increase of IIA from day 0 to 21 was more than 200-fold in control iPSCs, while a maximal 80-fold increase was seen in the mutant. The IIB form was up-regulated 25-fold in control iPSCs and 15-fold in *TRPV4*-iPSCs from day 0 to 21 (Figz. 3B). The stronger expression of form IIA compared

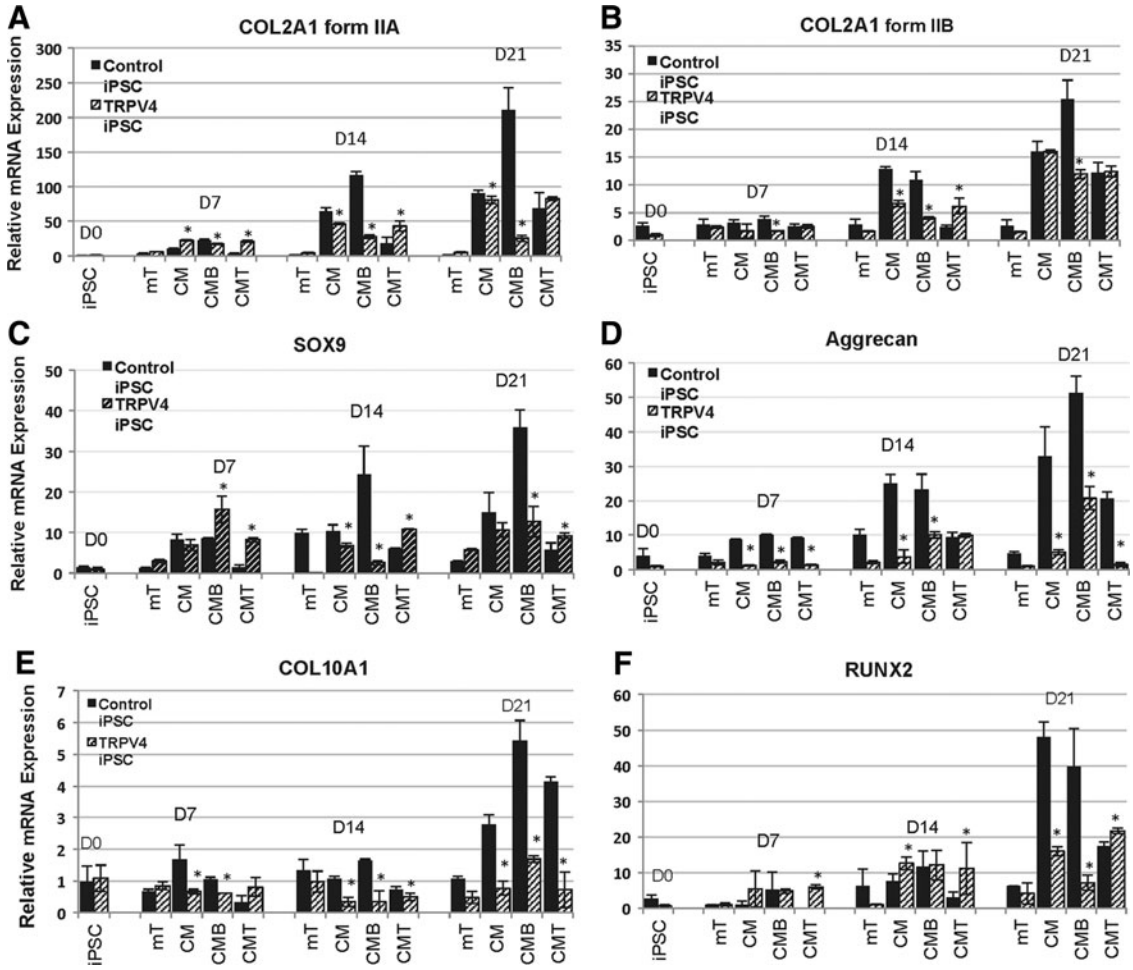

FIG. 3. Quantitative real-time polymerase chain reaction of chondrogenic marker mRNA expression at days 7, 14, and 21 in the iPSC micromass culture model. *COL2A1* encodes two main alternatively spliced forms (IIA and IIB) of this cartilage-specific extracellular matrix protein, type II collagen. In panel **A,** *COL2A1* form IIA is shown; while in panel **B**, *COL2A1* form IIB expression levels are shown. In panel **C**, the expression of *SOX9* is shown and *aggrecan* is seen in panel **D**. The two *bottom panels* demonstrate the expression of later chondrogenic stage markers, *COL10A1* of type X collagen **(E)**, and *RUNX2* **(F)**. Cultures were grown in mTeSR (mT) or CM, with *BMP2* (CMB) or with *TGFβ1* (CMT). The patterns of expression over time differ when comparing control iPSCs (*solid dark bars*) with mutant (*hatched bars*). Note differences in scale among panels representing fold expression relative to the internal control *GAPDH*. The bars represent data averaged from experiments performed in triplicate using control (83i-n1 and/or 14i-n6) and *TRPV4* (23i-n12 and/or 23i-n14) iPSC clones. Y-axis values represent fold difference. *Asterisks* indicate statistically significant differences ($P < 0.05$) between *TRPV4* compared with control iPSCs in chondrogenic conditions (CM, CMB, and CMT).

with form IIB suggests that early stages of chondrogenic differentiation are represented in our iPSC micromass model during this time frame in culture. Further, we found distinct differences between control and *TRPV4*-iPSCs in their response to *BMP2* (CMB) stimulation. As shown in Fig. 3A, a steady increased expression of *COL2A1* form IIA is observed when control iPSCs are treated with *BMP2* (CMB), while mutant *TRPV4*-iPSCs show a down-regulation of IIA when compared with CM. Overall, in control iPSCs, the strongest expression of IIA (about 120-fold at day 14 and 210-fold at day 21) was seen in the presence of *BMP2* (CMB). Instead in *TRPV4*-iPSCs, the highest expression of IIA (about 50-fold at day 14 and 80-fold at day 21) was observed in CM alone, and the addition of *BMP2* (CMB) at day 14 and 21 resulted in decreased expression of the IIA form. Similar effects of *BMP2* were seen on the expression of form IIB (Fig. 3B), which is up-regulated by *BMP2* (CMB) at 21 days in controls, but instead appears down-regulated in *TRPV4*-iPSCs.

A statistical analysis of *COL2A1* (form IIA and form IIB) expression at each time point and over time, with calculated *P* values of comparisons between control and *TRPV4*-iPSCs, was performed and compared only under chondrogenic conditions (CM, CMB, and CMT). Using an unpaired Student *t*-test and chi square test, we found that *COL2A1* IIA has significantly decreased expression in the *TRPV4* iPSCs at 7 ($P < 0.005$), 14 ($P < 0.0001$), and 21 ($P < 0.0005$) days, when compared with control iPSCs in CMB conditions. In addition, the IIB form in CMB was significantly ($P < 0.01$) decreased at 7 ($P < 0.005$), 14 ($P < 0.001$), and 21 ($P < 0.01$) days. However, the expression of form IIA at 21 days (in CMT but not in CM or CMB) and IIB (in CM and

CMT, but not in CMB) was comparable in control and *TRPV4* iPSCs. Since IIA and IIB are expressed at different stages of chondrogenesis [38], it is possible that the CMT and/or CM conditions have similar responses in both normal and mutant iPSCs. In addition, the observed increased ($P < 0.05$) expression in control iPSCs of *COL2A1* (IIA and IIB) in CMB, but decreased in CMT, when compared with their respective CM conditions at 7, 14, and 21 days, confirms the opposing effects of *BMP2* and *TGFβ1* during chondrogenesis as previously observed by others [40].

Together, these results suggest that *BMP2* stimulates *COL2A1* in control iPSCs, as expected [10,36,38], but acts aberrantly in *TRPV4*-iPSCs, resulting in the inhibition of *COL2A1* expression, rather than stimulation. These findings are of interest as in prechondrogenic tissue, IIA binds *BMP2* [36], and BMP signaling is required during condensation in prechondrogenic cells [54,55]. *COL2A1* is a cartilage-specific collagen gene that is usually up-regulated by BMP signaling through the transcription factor *SOX9*, a master regulator of chondrogenesis [56]. *SOX9* is required for cartilage formation [32] and for directing hypertrophic maturation of chondrocytes [33]. Here, qPCR of *SOX9* shows a significant ($P < 0.05$) increase of approximately 35-fold expression, in control iPSCs at day 21 when grown with *BMP2* (CMB); while in the same conditions, no increase was observed in *TRPV4*-iPSCs (Fig. 3C, CM vs. CMB). At day 7 in CMB, there appears to be higher expression in *TRPV4*-iPSCs, which may be due to abnormal regulation of its expression. It is possible that the maximum level of expression was reached at this time point and did not significantly increase at the later time points, as instead was seen in control iPSCs at 14 ($P < 0.05$) and 21 ($P < 0.005$) days, compared with their respective CM. This is in agreement with previously reported works showing that *TRPV4* regulates the *SOX9* pathway, contributing to the normal process of chondrogenesis [9].

Aggrecan, a marker of differentiated chondrocytes [38], shows significantly ($P < 0.005$) greater expression in controls (up to 50-fold in CMB) versus *TRPV4*-iPSC (up to 20-fold in CMB) over 21 days, with overall higher expression in control iPSCs also at 7 (CM, CMB, and CMT) and 14 days (mT, CM, and CMB), as shown in Fig. 3D. We also found, in *TRPV4* compared with control iPSCs, significantly decreased expression at day 7 ($P < 0.0001$) in CM, CMB, and CMT; at day 14 ($P < 0.005$) in CM and CMB; and at day 21 ($P < 0.005$) in CM, CMB, and CMT.

The expression of additional chondrogenic growth plate markers was tested, including *COL10A1* (Collagen X) shown in Fig. 3E and the transcription factor *RUNX2* seen in Fig. 3F. These last two molecules are specific for the hypertrophic zone of the growth plate [33]. We observed that while *COL10A1* and *RUNX2* were significantly ($P < 0.05$) up-regulated for approximately 6 (CMB) and 50 (CM) fold in controls at 21 days, respectively, a very modest increase for *COL10A1* (<2-fold, CMB) and about 20-fold for *RUNX2* (CMT) was seen in *TRPV4*-iPSCs (Fig. 3E, F). We noted statistically significant changes in *COL10A1* at day 7 ($P < 0.05$) in CM and CMB, and at 14 ($P < 0.05$) and 21 ($P < 0.05$) days in CM, CMB, and CMT. Significant changes were noted for *RUNX2* at day 21 ($P < 0.005$) in CM and CMB.

These data show that key late markers (*COL10A1* and *RUNX2*) of the cartilage growth plate are not expressed at similar levels in mutant iPSCs compared with controls, potentially impacting chondrocyte maturation [33]. *RUNX2* is a late marker of chondrogenesis and, as expected, has low levels of expression at 7 and 14 days of chondrogenic differentiation of the iPSC micromasses. This is the likely reason that there is no difference in the expression between control and *TRPV4* iPSCs for this marker at these early time points.

The findings may correlate with the severely reduced hypertrophic zone seen in the cartilage of lethal metatropic dysplasia patients, including the patient used for this study with a I604M mutation [5].

During endochondral ossification, BMP and TGFβ signaling pathways display antagonistic effects on chondrocyte proliferation and differentiation in vivo [40]. We also noted opposing effects of *TGFβ1* and *BMP2* on chondrogenic marker expression in both control and *TRPV4*-iPSCs (Fig. 3). Our iPSC model shows that the addition of *TGFβ1* (CMT) to control iPSCs resulted in significantly decreased expression of both *COL2A1* forms, IIA and IIB, at days 7 and 14 (Fig. 3A, B); of SOX9 at days 7, 14, and 21 (Fig. 3C); and of *Aggrecan* (Fig. 3D) and *RUNX2* (Fig. 3F) at days 14 and 21, when compared with their respective CM time points. However, in the presence of *BMP2*-supplemented medium (CMB), the earlier chondrogenic markers show up-regulation in control iPSCs (Fig. 3A–D, F). In *TRPV4*-iPSCs, the addition of *TGFβ1* (CMT) at 14 days did not produce a significant change in the level of expression of the earlier chondrogenic markers, while the addition of *BMP2* (CMB) resulted in down-regulation of *COL2A1* (both forms), *SOX9*, *COL10A1*, and *RUNX2* (Fig. 3A–C, E, F; CM vs. CMT or CMB). Instead, *Aggrecan* and *COL10A1* at 21 days were up-regulated in CMB, but not in CMT (Fig. 3D, E).

Overall, the qPCR data indicate that the necessary up-regulation of critical chondrogenic molecules, such as *SOX9*, *COL2A1* spliced form IIA, expressed in chondroprogenitor cells, and the hypertrophic marker *COL10A1*, are impaired in *TRPV4*-iPSCs at early stages of cartilage development. In addition, altered *BMP2* and *TGFβ1* signals are present in mutant iPSCs during chondrogenic differentiation in vitro. Finally, our iPSC model confirms that opposing effects of *BMP2* and *TGFβ1* on the regulation of chondrogenic marker expression are present.

Immunofluorescence and western blot assays confirm an abnormal production of the cartilage protein COL2 and the bone protein COL1 in TRPV4-*iPSC micromasses*

Next, studies at the protein level were consistent with the qPCR results (Fig. 3), showing that COL2 stains strongly in control iPSCs (Fig. 4A, top panels CM, CMB but not in mT or in CMT). In *TRPV4*-iPSC micromasses, weak staining was seen in CM and CMT, but no positive staining was seen in mT and CMB (Fig. 4A, bottom panels). We then compared micromass staining with human neonatal control cartilage sections (Fig. 4B, left panels) and with mutant *TRPV4* cartilage (Fig. 4B, right panels). Decreased staining for COL2 and decreased cell density (shown by less DAPI staining) was seen in the patient sample compared with control cartilage. DAPI- and COL2-positive cells were counted in triplicate for both control and patient samples.

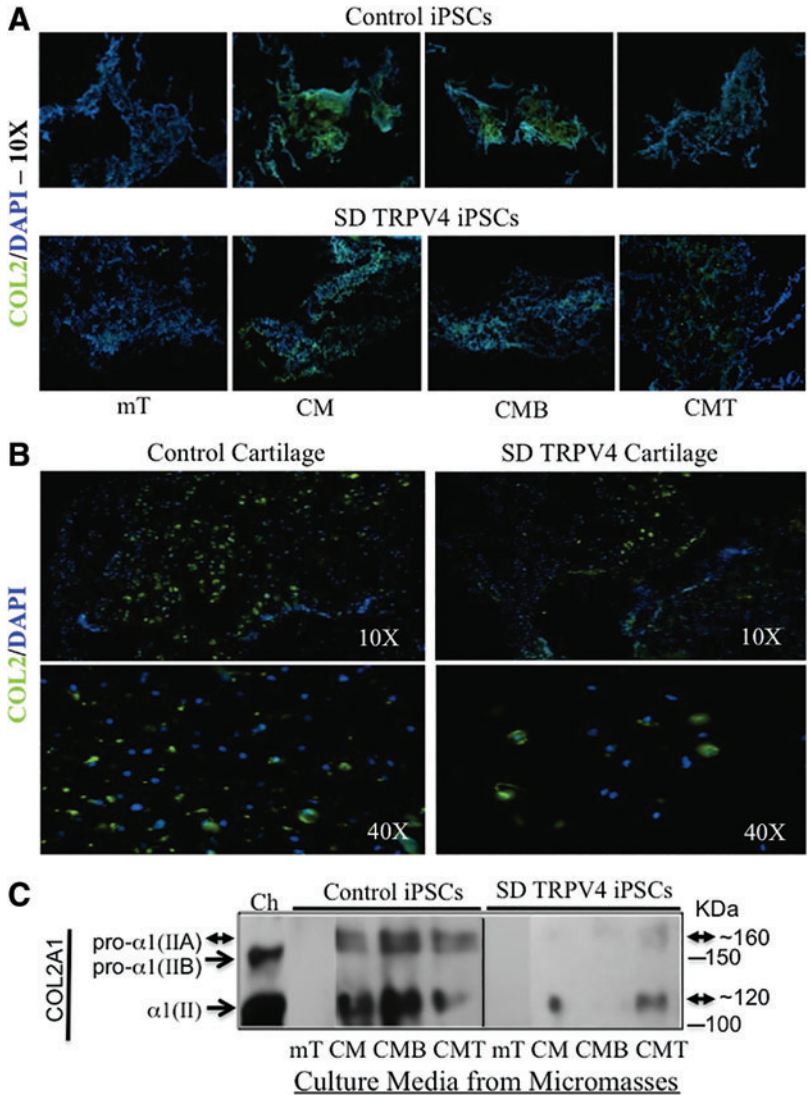

FIG. 4. Immunofluorescence microscopy and western blot analysis of iPSC micromass cultures and human neonatal cartilage for type II collagen (COL2) protein expression. Primary anti-human *COL2A1* monoclonal antibody (Ab300, Abcam) with secondary Alexa-Fluor 488 antibody staining (*green*) is shown in panels **A** and **B**. The slides were counterstained with DAPI staining nuclei (*blue*). In panel **A,** micromasses from control 83i (*top*) and 23i-n14 (*bottom*) iPSCs stained for *COL2A1* are displayed; while panel **B** shows cartilage sections from the control (*left panels*) and the SD *TRPV4* patient (*right panels*) stained for type II collagen (COL2). In panel **C**, western blot analysis of proteins secreted in the media of each micromass culture at day 21 is shown. Since COL2 is composed of $[\alpha1(II)]_3$ chains, and is a secreted extracellular matrix protein, no internal protein standard was used, but the same amount of media (30 μL) in the presence of beta-mercaptoethanol (BME) was loaded for the control (83i-n1) and the SD *TRPV4* (23i-n14) iPSC lines under each condition. Procollagen, pro-α1(IIA) of 1,487 amino acids (aa) shown at ~170 kDa and its mature isoform α1(II) of 1,060 aa (~120 kDa) are present in iPSCs as indicated by *double arrowheads*. The procollagen pro-α1(IIB) of 1,418 aa is seen at ~150 kDa (*arrowhead*), a form excluding protein-coding exon 2, and is only seen in the control, normal human chondrocytes (Ch) grown in CM. Its mature isoform is α1(II) of 1,060 aa at ~120 kDa (*arrowhead*). This processed isoform has the same kDa size and amino-acid sequence of the mature α1(II) isoform of ~120 kDa (*double arrowheads*) generated from pro-α1(IIA). This occurs after cleavage of the N-propeptides removing the region of exon 2. All the isoforms have post-translational modification, resulting in an increased mass [52]. The proteins were separated using 4%–12% gradient SDS-PAGE, transferred, and probed with α1(II) monoclonal antibody 3092 (Abcam). Experiments were also performed using control (14i-n6) and SD *TRPV4* iPSC (23i-n12) clones with similar results (not shown). Protein markers at 100 and 150 kDa are indicated. Color images available online at www.liebertpub.com/scd

The results showed 62% fewer cells in patient cartilage compared with control cartilage, but the overall ratio of COL2-positive cells was very similar (~40%).

Western blot of culture media collected from the different micromass conditions assessed secreted proteins and showed that the cartilage-specific chondroprogenitor form of COL2, the unprocessed pro-collagen alpha IIA [pro-α1(IIA)] chain, was secreted and detected in both control and *TRPV4*-iPSCs (Fig. 4C, CM, CMB, and CMT). However, there were weaker bands of pro-α1(IIA), shown at ~160 kDa, and in its

processed form α1(II), of ~120 kDa, in *TRPV4*-iPSCs versus those of control iPSCs. In the presence of *BMP2* (CMB), the α1(II) processed form of pro-α1(IIA) was almost undetectable, while a strong intense band (also at ~120 kDa) was seen in controls (CMB), confirming the qPCR data of inhibition of *COL2A1*-IIA expression in *TRPV4*-iPSCs and its up-regulation in controls (Fig. 3A, CMB). No *COL2A1* bands for pro-α1(IIA), pro-α1(IIB) or their identical processed form α1(II) were seen in mT, as seen at the mRNA level by qPCR (Fig. 3A, C, mT). In addition, no bands were seen for pro-α1(IIB) in either control or *TRPV4*-iPSCs, probably due to the very low expression of form IIB (Fig. 3C). In contrast, in the culture media from primary human chondrocytes (Ch) used as a control, we detected the

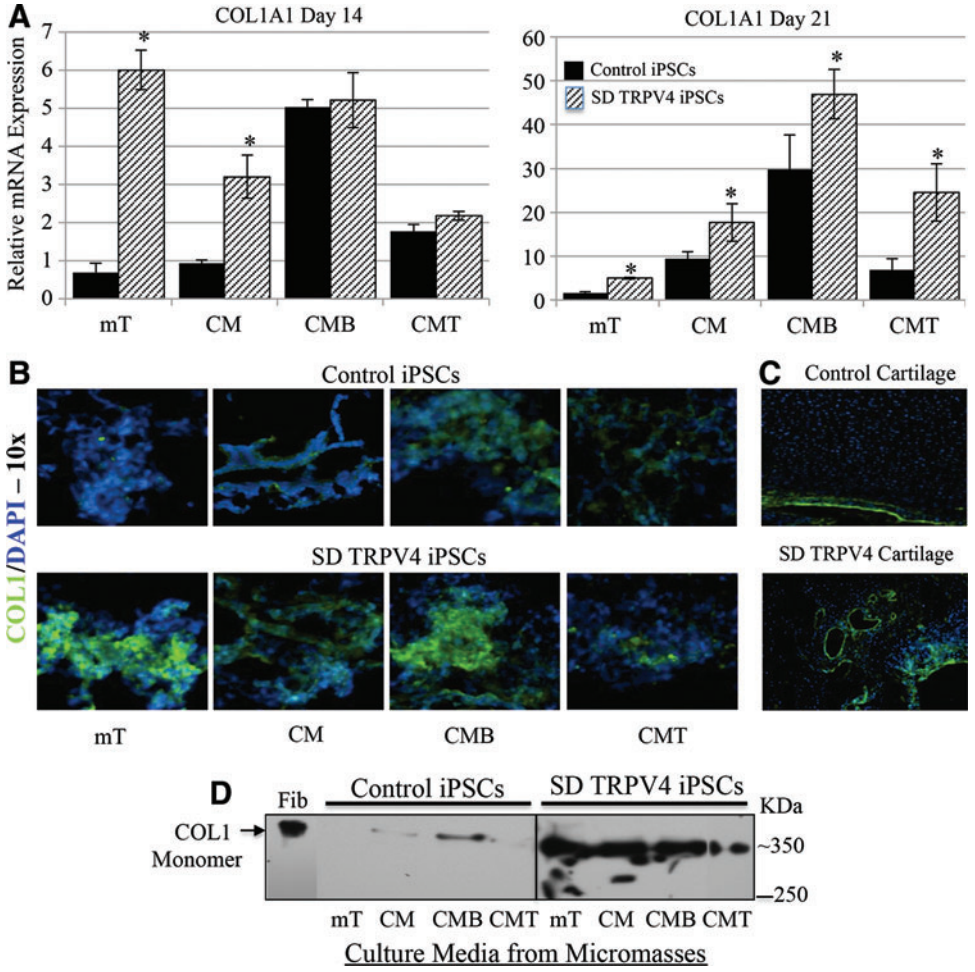

FIG. 5. *COL1A1* mRNA and protein expression at days 14 and 21 in the iPSC micromass culture model using qPCR, immunofluorescence microscopy, and western blot analysis of type I collagen (COL1). **(A)** RT-PCR using specific primers for *COL1A1* (Supplementary Table S1), in iPSC chondrogenic micromass cultures at day 14 and 21. Note difference in scale. Expression levels for control iPSC are shown as *black bars*, while expression for mutant SD *TRPV4* iPSCs is shown with *hatched bars*. Micromasses were grown in the various described media, control (mT), CM, CMB, and CMT. Experiments were run in triplicate using control 83i-n1 and *TRPV4* iPSC clones. Y-axis values represent fold difference. **(B)** Indirect immunofluorescence microscopy of the micromasses for control (83i-n1) and SD *TRPV4* (23i-n14) iPSC clones grown in the different media for 21 days. Staining is shown using an antibody against *COL1A1* (*green*) with DAPI counterstaining (*blue*) showing nuclei. Control micromasses are seen in the *upper panels*, while the *TRPV4* iPSCs are shown in the *lower panels*. Experiments were also performed using control (83i-n1 and/or 14i-n6) and *TRPV4* (23i-n12 and/or 23i-n14) iPSC clones. All magnifications are 10×. **(C)** displays human neonatal cartilage sections stained for *COL1A1* (*green*) and DAPI (*blue*) with sections from a normal control in the upper photomicrograph and from the patient with *TRPV4* mutation in the lower micrograph. **(D)** Western blot analysis of the micromass iPSC culture media at day 21 using an antibody to the mature monomer form of type I collagen (COL1) composed of the $[\alpha1(I)]_2$ $[\alpha2(I)]$ chains. The antibody, therefore, detects the native monomer protein with both assembled chains at ~350 kDa. The difference in band migration between control fibroblasts (Fib) and iPSC lines may reflect differential post-translational modification and processing. COL1 is an extracellular matrix-secreted protein; thus, internal controls such as b-actin or *GAPDH* were not used, but the same amount of media (30 μL) in the absence of BME was loaded for each condition and iPSC line. Control normal human fibroblasts (Fib) were used as a positive control. Proteins were separated using 4%–12% gradient SDS-PAGE, transferred, and probed with the COL1 polyclonal antibody 600-401 (Rockland). A protein marker of 250 kDa is indicated. *Asterisks* indicate $P < 0.05$ by Student's *t*-test. Color images available online at www.liebertpub.com/scd

unprocessed form pro-α1(IIB), but not pro-α1(IIA), shown at ~150 kDa and its cleaved form α1(II) at ~120 kDa (Fig. 4C, Ch), as expected for mature differentiated chondrocytes [36,38,57]. Overall, immunofluorescence staining from micromasses and western blot data using micromass culture media for COL2 confirm at the protein level, the abnormal regulation of *COL2A1* expression in *TRPV4*-iPSCs, seen by qPCR assays. We also found that *BMP2* and *TGFβ1* signaling, two key regulators of chondrogenesis [39,40], is abnormal in iPSCs derived from the SD *TRPV4* patient with lethal metatropic dysplasia (Figs. 3 and 4).

We found that (i) *TRPV4*-iPSC micromasses showed abnormal Alcian blue staining and for Alizarin red (also present in the cartilage of the *TRPV4* patient) when compared with controls (Fig. 2); (ii) the hypertrophic chondrogenic marker *COL10A1* and the transcription factor *RUNX2*, highly expressed during the late stages of chondrogenesis before ossification [37,38] were down-regulated in *TRPV4*-iPSC clones but not in control lines (Fig. 3); and (iii) COL2 protein secretion was significantly reduced and dysregulated by *BMP2* and *TGFβ1* in patient-derived iPSCs (Fig. 4). To better understand the significance of these findings, we examined the expression of type I collagen (COL1), the major collagen of bone [58]. COL1 is a heterotrimer molecule formed by two identical α1 chains and one α2 chain [$\alpha1_2$(I) α2(I)], with slightly different amino-acid sequences. We found abnormal expression and staining of COL1 in *TRPV4*-iPSCs and in the neonatal cartilage sections of patient tissue compared with controls, respectively (Fig. 5). Analysis by qPCR of iPSC chondrogenic micromass at day 14 (mT and CM) showed significantly ($P < 0.05$) increased expression of *COL1A1* in *TRPV4*-iPSCs when compared with control iPSCs and also at day 21 in all media tested (Fig. 5A). *COL1A1* is a late marker of chondrogenesis; as expected, has low levels of expression at day 14 compared with day 21; and probably is not yet regulated by the addition of *BMP2* (CMB) or *TGFβ1* (CMT), as we instead observed at 21 days of chondrogenic differentiation of the iPSC micromasses. This is the most likely reason that there is no difference in the expression between control and *TRPV4* iPSCs in the earlier conditions for this marker at the 14 day timepoint. Of note, even in nonchondrogenic media (mT), this difference between control and *TRPV4* iPSCs was seen at both time points (Fig. 5A, mT).

Figure 5B compares immunofluorescence staining *COL1A1* (green) and nuclei (blue) of the micromasses grown in the various media for 21 days, and stronger staining of this osteogenic marker in all conditions (mT, CM, CMB, and CMT) was observed in the *TRPV4*-iPSCs compared with the control (Fig. 5B). Figure 5C shows human neonatal cartilage sections stained for *COL1A1* (green) and nuclei (blue). The control seen in the upper image shows that *COL1A1* staining is confined to the peripheral zone; while in the patient cartilage sections, ''islands'' of *COL1A1* staining are seen. This is consistent with Alizarin red staining for developing bone (Fig. 2D) and further supports the concept that developmental progression of chondrogenesis and osteogenesis is abnormal with a mutation in *TRPV4*. Figure 5D shows western blot data of secreted protein from the iPSC micromass culture media at day 21. The antibody detects the secreted and assembled monomer of the COL1 heterotrimer native protein. The monomer of COL1 with both chains at ~350 kDa is detected in nondenaturing conditions (as described in Material and Methods), using the same antibody employed for the immunofluorescence (Fig. 5B, C), and stronger bands were noted in *TRPV4*-iPSCs media compared with the control. These findings are in agreement with the significantly increased expression of *COL1A1* (Fig. 5A) and increased staining for COL1 observed in *TRPV4*-iPSCs (Fig. 5B, bottom panel) compared with the control (Fig. 5B, top panel).

Discussion

The iPSC technique reprograms differentiated cells (fibroblasts and others) to a pluripotent state for induction toward a chosen tissue [59]. This enables recapitulation of the biochemical and molecular pathways of that tissue at early developmental stages to model human disease in the culture dish [17,60]. We developed an iPSC model that is capable of recapitulating developmental markers of chondrogenesis from the early steps of mesenchymal cell condensation and confirmed the data at the mRNA and protein levels. The *BMP2* and *TGFβ1* signaling pathways appear to be recapitulated in the control iPSCs but show abnormal signaling in the patient-derived iPSCs. We compared the actual patient's cartilage and control to validate our findings in the chondrogenic-induced iPSC micromasses derived from this same patient's fibroblasts. We found that the patient cartilage showed irregular Alcian blue and Alizarin red staining compared with the control cartilage. This finding supports the abnormal staining observed in the chondrogenic micromasses of the mutated iPSC lines.

Specifically, we studied the effects of a mutation (I604M) causing lethal metatropic dysplasia, the most severe known phenotype of *TRPV4* mutations. Published data do not demonstrate a strict genotype:phenotype correlation in SD-*TRPV4* disorders [5,6], raising the question of why some mutations are lethal while others are not. Earlier studies showed that both lethal and nonlethal mutations constitutively activate the *TRPV4* calcium channel, suggesting that increased calcium influx affects normal cartilage formation but they were unable to quantitatively correlate them to disease severity [3–5]. However, a recent report suggests a strong correlation between increased basal activity and severity of SD caused by *TRPV4* mutations [12]. These opposing findings could be explained by the use of different cellular models and/or their limitations in studying *TRPV4* activity, as they are transfection models resulting in overexpressed homotetrameric mutant channels [3–7,12]. Instead, the chondrogenic iPSC model enables us to study the natural heterozygous state of the mutation, where the majority of channels likely reflect a composite of normal and mutant chains [13,61]. This approach provides a true genetic model of this disorder and the opportunity to discern the effects of a heterozygous mutation during chondrogenic differentiation.

To verify that early stages of chondrogenesis were represented in our model, we used qPCR to examine the differentially spliced form IIA of COL2, a cartilage-specific protein, expressed during vertebral development in distinct cells surrounding the cartilage [53], and deposited in the extracellular matrix of prechondrogenic tissue [36]. Our data indicate that the necessary up-regulation of this important

marker of chondrogenesis is impaired in the *TRPV4* mutant. Recently characterized homozygous *Col2a1*$^{+ex2}$ knock-in mice, where the IIA form is exclusively expressed, showed that cartilage tissue assembled into thin-banded fibrils [57], indicating that functional cartilage can be formed with only the IIA form of COL2 [62]. In addition, the relatively higher expression of IIA compared with IIB suggests that early, rather than late, stages of chondrogenesis are represented in our iPSC model during this time frame in culture.

The long bones of the limbs, vertebrae, and ribs develop through endochondral ossification [63], where prechondrogenic mesenchyme condensation triggers the steps of chondrogenic differentiation, forms cartilage [38,56], and is affected in SDs [1]. In vitro and in vivo studies have shown that BMP signaling plays a central role in the formation of precartilaginous condensations and in the differentiation of chondroprogenitors into chondrocytes [64]. Studies of conditional knockout mice showed that *BMP2*, but not BMP4, was critical for chondrocyte proliferation and maturation during endochondral development [65]. The mice exhibited extensive disorganization of chondrocytes within the growth plate and defects in chondrocyte proliferation, resulting in a severe chondrodysplasia phenotype. In addition, very recently, it was shown that *TRPV4* expression is under the control of *BMP2* during osteoblast differentiation of primary osteoblast-enriched cell cultures [66], and that bone marrow- and adipose-derived mesenchymal stem cells from *Trpv4*-deficient mice have an altered adipogenic, osteogenic, and chondrogenic differentiation potential [67].

When we examined *BMP2* in our system, we found distinct differences in the response to *BMP2* stimulation. Control iPSCs treated with *BMP2* showed a significant increase of form IIA of COL2, as well as form IIB at 21 days, while the mutant *TRPV4*-iPSCs showed down-regulation. Overall, *BMP2* is expected to show a stimulatory effect on *COL2A1* expression [10,36,39] that was seen in control iPSCs, but an inhibitory outcome was reproduced in our *TRPV4*-iPSCs. These findings are of interest as in prechondrogenic tissue, IIA binds *BMP2* [36]. *BMP2* in normal human iPSCs and in iPSC-derived mesenchymal stem cells was shown to promote chondrogenic differentiation by the enrichment of *COL2A1* [31], consistent with our data. Further, BMP signaling in prechondrogenic cells and in growth plate chondrocytes stimulates *SOX9, COL2A1,* and *COL10A1,* molecules that are progressively associated with chondrogenic differentiation and maturation toward hypertrophic chondrocytes [37,56].

We found that mutant iPSCs treated with *BMP2* lack increased expression of *SOX9, COL2A1, COL10A1,* and *RUNX2* over time. This increase was observed in control iPSCs, suggesting that an aberrant BMP2 signal could be related to abnormal chondrogenesis. *SOX9*, in particular, is considered a master regulator of chondrogenesis and directly stimulates COL10 expression in maturing chondrocytes [32,33]. In vitro studies of mouse mesenchymal cells transiently transfected with normal mouse *TRPV4* cDNA showed increased levels of *SOX9*-dependent reporter activity, and increased steady-state levels of *SOX9* mRNA [9]. The authors concluded that *TRPV4* regulates the *SOX9* pathway, contributing to the process of chondrogenesis. Their data validate, to some extent, our *TRPV4*-iPSC model as no increased expression of *SOX9* was observed over time in the mutant, as was seen in control iPSCs. However, since no mutant *TRPV4* cDNA was used in the published mouse study, our results cannot be fully compared with their findings. When we tested *COL10A1* and the transcription factor *RUNX2*, both of which were specific for the hypertrophic zone [33], and late-stage markers, we observed that both were significantly increased in controls but not in *TRPV4*-iPSCs at the later days in culture, suggesting failure of the mutant iPSCs to progress through these later stages of growth plate development.

Studies show that during endochondral ossification, BMP and TGFβ signaling pathways can have antagonistic effects on chondrocyte proliferation and differentiation in vivo and on prechondrogenic condensation in vitro, showing that TGFβ signaling can inhibit chondrocyte proliferation and differentiation of proliferating chondrocytes to hypertrophic chondrocytes, while *BMP2* has opposite effects [40]. We also found that while *TGFβ1* in control iPSCs resulted in decreased expression of *COL2A1* IIA and IIB, *SOX9*, *Aggrecan*, and *RUNX2* in *TRPV4*-iPSCs, the addition of *TGFβ1* did not produce a significant change. We also confirmed this at the protein level for COL2, showing that *BMP2* and *TGFβ1* have opposing effects on key cartilage and bone marker expression during early stages of in vitro chondrogenesis. Of note, the addition of *BMP2* led to almost undetectable COL2 secretion in *TRPV4*-iPSCs, while the *TGFβ1* treated micromasses were unaffected. Taken together, these results indicate that the patient-derived iPSC model appropriately recapitulates multiple sequential molecular markers of human growth plate development.

To further explore the abnormal mineralization detected by Alizarin red, we studied expression of type I collagen, the major structural matrix protein of bone [58]. Interestingly collagen I (*COL1A1*), an osteogenic marker restricted to the perichondrium when the process of endochondral ossification is advanced [63], showed significantly higher expression in *TRPV4*-iPSCs compared with the control at 14 and 21 days with or without the addition of growth factors. In addition, *COL1A1* was the only marker increased in the presence of *BMP2* at 21 days in the disease iPSC model; while all the others (*COL2A1, SOX9, Aggrecan, COL10A1,* and *RUNX2*) were at significantly lower levels compared with control iPSCs. Together, the mRNA expression data correlate with the western and immunofluorescence data from the micromasses showing aberrantly increased COL1 expression and an abnormally decreased response of COL2 to *BMP2* under chondrogenic induction in the *TRPV4*-iPSCs.

In summary, our data suggest that *TRPV4* mutation causing lethal metatropic dysplasia disrupts the normal sequence of differentiation which occurs during endochondral bone formation, showing inappropriate expression of COL1, a marker typical of late stages of chondrogenesis with very low expression of the earlier markers of growth plate formation [38]. For example, *SOX9*, a crucial regulator of chondrogenesis that controls COL2 expression, directs the maturation of hypertrophic chondrocytes and blocks osteoblast differentiation of the growth plate [33], was inadequately expressed in the mutant iPSCs. It is possible that the abnormally high COL1 expression in *TRPV4*-IPSCs reflects premature initiation of bone differentiation, precluding normal growth plate and chondrocyte development. This

hypothesis would correlate with the shortened and immature growth plates seen in this disorder [5], but requires further directed investigation.

This work describes the first development of an iPSC chondrogenic model of SD, an in vitro demonstration that abnormal processes can be investigated at the molecular level. A major limitation in the field of cartilage biology is the availability of primary cultured cells that maintain a chondrogenic phenotype during expansion. Our novel approach reflects the disease state in the appropriate developing cell type and enables analysis of critical chondrogenic regulators across a phenotypic spectrum of this disorder, laying the foundation for targeted therapies. The advancement of a human ''disease in a dish'' model system reflects a major improvement in the field and creates a novel paradigm to answer key questions in cartilage development and disease.

Acknowledgments

This study was supported in part by funds from the Medical Genetics Institute and the Regenerative Medicine Institute at the Cedars-Sinai Medical Center, the Broad Stem Cell Research Center, the Orthopedic Institute for Children and the Orthopedic Hospital Research Center at UCLA, the ISDR, grants from the National Institutes of Health (DE019567 and AR062651 to D.H.C.), and the National Center for Advancing Translational Sciences, grant UL1TR000124. The content is solely the responsibility of the authors and does not necessarily represent the official views of the NIH. The authors also wish to thank the iPSC core for their assistance in generating the *TRPV4*-iPSCs, the Cedars-Sinai Genomics Core and Cytogenetics Core for the qPCR and the fluorescence microscopy, respectively, and Lisette Nevarez at UCLA for sequencing the iPSC clones. The authors would like to thank William Wilcox and Michael Weinstein for helpful discussions and Sulagna C. Saitta for a critical reading of this article.

Author Disclosure Statement

The authors declare no conflict of interest. No competing financial interests exist.

References

1. Krakow D and D Rimoin. (2010). The skeletal dysplasias. Genet Med 12:327–341.
2. Kronenberg H. (2003). Developmental regulation of the growth plate. Nature 423:332–336.
3. Rock MJ, J Prenen, VA Funari, TL Funari, B Merriman, SF Nelson, RS Lachman, WR Wilcox, S Reyno, et al. (2008). Gain-of-function mutations in TRPV4 cause autosomal dominant brachyolmia. Nat Genet 40:999–1003.
4. Krakow D, J Vriens, N Camacho, P Luong, H Deixler, TL Funari, CA Bacino, MB Irons, IA Holm, et al. (2009). Mutations in the gene encoding the calcium-permeable ion channel TRPV4 produce spondylometaphyseal dysplasia, Kozlowski type and metatropic dysplasia. Am J Hum Genet 84:307–315.
5. Camacho N, D Krakow, S Johnykutty, PJ Katzman, S Pepkowitz, J Vriens, B Nilius, BF Boyce and D Cohn. (2010). Dominant TRPV4 mutations in nonlethal and lethal metatropic dysplasia. Am J Med Genet 152A:1169–1177.
6. Nishimura G, J Dai, E Lausch, S Unger, A Megarbané, H Kitoh, OH Kim, TJ Cho, F Bedeschi, et al. (2010). Spondylo-epiphyseal dysplasia, Maroteaux type (pseudo-Morquio syndrome type 2), and parastremmatic dysplasia are caused by TRPV4 mutations. Am J Med Genet A 152A:1443–1449.
7. Lamande SR, Y Yuan, IL Gresshoff, L Rowley, D Belluoccio, K Kaluarachchi, CB Little, E Botzenhart, K Zerres, et al. (2011). Mutations in TRPV4 cause an inherited arthropathy of hands and feet. Nat Genet 43:1142–1146.
8. Nishimura G, E Lausch, R Savarirayan, M Shiba, J Spranger, B Zabel, S Ikegawa, A Superti-Furga and S Unger. (2012). TRPV4-associated skeletal dysplasias. Am J Med Genet C Semin Med Genet 160C:190–204.
9. Muramatsu S, M Wakabayashi, T Ohno, K Amano, R Ooishi, T Sugahara, S Shiojiri, K Tashiro, Y Suzuki, et al. (2007). Functional gene screening system identified TRPV4 as a regulator of chondrogenic differentiation. J Biol Chem 282:32158–32167.
10. Cameron TL, D Belluoccio, PG Farlie, B Brachvogel and J Bateman. (2009). Global comparative transcriptome analysis of cartilage formation in vivo. BMC Dev Biol 9:20–29.
11. Everaerts W, B Nilius and K Owsiani. (2010). The vanilloid transient receptor potential channel TRPV4: from structure to disease. Prog Biophys Mol Biol 103:2–17.
12. Loukin S, Z Su and C Kung. (2011). Increased basal activity is a key determinant in the severity of human skeletal dysplasia caused by TRPV4 mutations. PLoS One 6:e19533.
13. Nilius B and T Voets. (2013). The puzzle of TRPV4 channelopathies. EMBO Rep 14:152–163.
14. Takahashi K and S Yamanaka. (2006). Induction of pluripotent stem cells from mouse embryonic and adult fibroblast cultures by defined factors. Cell 126:663–676.
15. Takahashi K, K Tanabe, M Ohnuki, M Narita, T Ichisak, K Tomoda and S Yamanaka. (2007). Induction of pluripotent stem cells from adult human fibroblasts by defined factors. Cell 131:861–872.
16. Yu J, MA Vodyanik, K Smuga-Otto, J Antosiewicz-Bourget, JL Frane, S Tian, J Nie, GA Jonsdottir, V Ruotti, et al. (2007). Induced pluripotent stem cell lines derived from human somatic cells. Science 318:1917–1920.
17. Soldner F and R Jaenisch. (2012). iPSC disease modeling. Science 338:1155–1156.
18. Beltrão-Braga PC, GC Pignatari, FB Russo, IR Fernandes and A Muotri. (2013). In-a-dish: induced pluripotent stem cells as a novel model for human diseases. Cytometry A 83:11–17.
19. Dimos JT, KT Rodolfa, KK Niakan, LM Weisenthal, H Mitsumoto, W Chung, GF Croft, G Saphier, R Leibel, et al. (2008). Induced pluripotent stem cells generated from patients with ALS can be differentiated into motor neurons. Science 321:1218–1221.
20. Sareen D, JG O'Rourke, P Meera, AK Muhammad, S Grant, M Simpkinson, S Bell, S Carmona, L Ornelas, et al. (2013). Targeting RNA Foci in iPSC-derived motor neurons from ALS patients with a C9ORF72 repeat expansion. Sci Transl Med 5:208ra149.
21. Park IH, N Arora, H Huo, N Maherali, T Ahfeldt, A Shimamura, MW Lensch, C Cowan, K Hochedlinger and G Daley. (2008). Disease-specific induced pluripotent stem cells. Cell 134:877–886.
22. Soldner F, D Hockemeyer, C Beard, Q Gao, GW Bell, EG Cook, G Hargus, A Blak, O Cooper, et al. (2009).

Parkinson's disease patient-derived induced pluripotent stem cell free of viral reprogramming factors. Cell 136: 964–977.
23. Ebert AD, J Yu, FF Rose Jr., VB Mattis, CL Lorson, JA Thomson and C Svendsen. (2009). Induced pluripotent stem cells from a spinal muscular atrophy patient. Nature 457:277–280.
24. Quarto N, B Leonard, S Li, M Marchand, E Anderson, B Behr, U Francke, R Reijo-Pera, E Chiao and M Longaker. (2012). Skeletogenic phenotype of human Marfan embryonic stem cells faithfully phenocopied by patient-specific induced-pluripotent stem cells. Proc Natl Acad Sci U S A 109:215–220.
25. Deyle DR, IF Khan, G Ren, PR Wang, J Kho, U Schwarze and DW Russell. (2012). Normal collagen and bone production by gene-targeted human osteogenesis imperfecta iPSCs. Mol Ther 1:204–213.
26. Diekman BO, N Christoforou, VP Willard, H Sun, J Sanchez-Adams, KW Leong and F Guilak. (2012). Cartilage tissue engineering using differentiated and purified induced pluripotent stem cells. Proc Natl Acad Sci U S A 20:19172–19177.
27. Oldershaw RA, MA Baxter, ET Lowe, N Bates, LM Grady, F Soncin, DR Brison, TE Hardingham and SJ Kimber. (2010). Directed differentiation of human embryonic stem cells toward chondrocytes. Nat Biotechnol 28:1187–1194.
28. Gong G, D Ferrari, CN Dealy and RA Kosher. (2010). Direct and progressive differentiation of human embryonic stem cells into the chondrogenic lineage. J Cell Physiol 224:664–671.
29. Medvedev SP, EV Grigor'eva, AI Shevchenko, AA Malakhova, EV Dementyeva, AA Shilov, EA Pokushalov, AM Zaidman, MA Aleksandrova, et al. (2011). Human induced pluripotent stem cells derived from fetal neural stem cells successfully undergo directed differentiation into cartilage. Stem Cells Dev 20:1099–1112.
30. Wei Y, W Zeng, R Wan, J Wang, Q Zhou, S Qiu and SR Sing. (2012). Chondrogenic differentiation of induced pluripotent stem cells from osteoarthritic chondrocytes in alginate matrix. Eur Cell Mater 23:1–12.
31. Guzzo RM, J Gibson, RH Xu, FY Lee and H Drissi. (2013). Efficient differentiation of human iPSC-derived mesenchymal stem cells to chondroprogenitor cells. J Cell Biochem 114:480–490.
32. Bi W, JM Deng, Z Zhang, RR Behringer and B Crombrugghe. (1999). Sox9 is required for cartilage formation. Nat Genet 22:85–89.
33. Dy P, W Wang, P Bhattaram, Q Wang, L Wang, RT Ballock and V Lefebvre. (2012). Sox9 directs hypertrophic maturation and blocks osteoblast differentiation of growth plate chondrocytes. Dev Cell 22:597–609.
34. Uitto J. (1977). Biosynthesis of type II collagen. Removal of amino-and carboxy-terminal extensions from procollagen synthesized by chick embryo cartilage cells. Biochemistry 16:3421–3429.
35. Ryan MC and L Sandell. (1990). Differential expression of a cysteine-rich domain in the amino-terminal propeptide of type II (cartilage) procollagen by alternative splicing of mRNA. J Biol Chem 265:10334–10339.
36. Zhu Y, A Oganesian, DR Keene and L Sandell. (1999). Type IIA procollagen containing the cysteine-rich amino propeptide is deposited in the extracellular matrix of prechondrogenic tissue and binds to TGF-beta1 and BMP-2. J Cell Biol 144:1069–1080.
37. Lefebvre V and P Smits. (2005). Transcriptional control of chondrocyte fate and differentiation. Birth Defects Res C Embryo Today 75:200–212.
38. Goldring MB, K Tsuchimochi and K Ijiri. (2006). The control of chondrogenesis. J Cell Biochem 97:33–44.
39. Yoon BS and K Lyons. (2004). Multiple functions of BMPs in chondrogenesis. J Cell Biochem 93:93–103.
40. Keller B, T Yang, Y Chen, E Munivez, T Bertin, B Zabel and B Lee. (2011). Interaction of TGFβ and BMP signaling pathways during chondrogenesis. PLoS One 6:16421e.
41. Fortier LA, JU Barker, EJ Strauss, TM McCarrel and B Cole. (2011). The role of growth factors in cartilage repair. Clin Orthop Relat Res 469:2706–2715.
42. Joyce NC, DL Harris, V Markov, Z Zhang and B Saitta. (2012). Potential of human umbilical cord blood mesenchymal stem cells to heal damaged corneal endothelium. Mol Vis 18:547–564.
43. Okita K, Y Matsumura, Y Sato, A Okada, A Morizane, S Okamoto, H Hong, M Nakagawa, K Tanabe, et al. (2011). A more efficient method to generate integration-free human iPS cells. Nat Methods 8:409–412.
44. Sareen D, AD Ebert, BM Heins, JV McGivern, L Ornelas and C Svendsen. (2012). Inhibition of apoptosis blocks human motor neuron cell death in a stem cell model of spinal muscular atrophy. PLoS One 7:e39113.
45. Baldassarre G, A Romano, F Armenante, M Rambaldi, I Paoletti, C Sandomenico, S Pepe, S Staibano, G Salvatore, et al. (1997). Expression of teratocarcinoma-derived growth factor-1 (TDGF-1) in testis germ cell tumors and its effects on growth and differentiation of embryonal carcinoma cell line NTERA2/D1. Oncogene 15:927–936.
46. Markov V, K Kusumi, MG Tadesse, DA William, DM Hall, V Lounev, A Carlton, J Leonard, RI Cohen, EF Rappaport and B Saitta. (2007). Identification of cord blood-derived mesenchymal stem/stromal cell populations with distinct growth kinetics, differentiation potentials, and gene expression profiles. Stem Cells Dev 16:53–73.
47. Toh WS, Z Yang, H Liu, BC Heng, EH Lee and T Cao. (2007). Effects of culture conditions and bone morphogenetic protein 2 on extent of chondrogenesis from human embryonic stem cells. Stem Cell 4:950–960.
48. Müller FJ, BM Schuldt, R Williams, D Mason, G Altun, EP Papapetrou, S Danner, JE Goldmann, A Herbst, et al. (2011). A bioinformatic assay for pluripotency in human cells. Nat Methods 8:315–317.
49. Ludwig T and A Thomson. (2007). Defined, feeder-independent medium for human embryonic stem cell culture. Curr Protoc Stem Cell Biol Chapter 1:Unit 1C.2.
50. Gay SW and R Kosher. (1984). Uniform cartilage differentiation in micromass cultures prepared from a relatively homogeneous population of chondrogenic progenitor cells of the chick limb bud: effect of prostaglandins. J Exp Zool 232:317–26.
51. Gregory CA, WG Gunn, A Peister and D Prockop. (2004). An Alizarin red-based assay of mineralization by adherent cells in culture: comparison with cetylpyridinium chloride extraction. Anal Biochem 329:77–84.
52. Fertala A, AL Sieron, Y Hojima, A Ganguly and D Prockop. (1994). Self-assembly into fibrils of collagen II by enzymic cleavage of recombinant procollagen II. Lag period, critical concentration, and morphology of fibrils differ from collagen I. J Biol Chem 269:11584–11589.
53. Sandell LJ, N Morris, JR Robbins and M Goldring. (1991). Alternatively spliced type II procollagen mRNAs define

distinct populations of cells during vertebral development: differential expression of the amino-propeptide. J Cell Biol 114:1307–1319.
54. Pizette S and L Niswander. (1999). BMPs negatively regulate structure and function of the limb apical ectodermal ridge. Development 126:883–894.
55. Chimal-Monroy J, J Rodriguez-Leon, JA Montero, Y Gañan, D Macias, R Merino and J Hurle. (2003). Analysis of the molecular cascade responsible for mesodermal limb chondrogenesis: Sox genes and BMP signaling. Dev Biol 257:292–301.
56. Pogue R and K Lyons. (2006). BMP signaling in the cartilage growth plate. Curr Top Dev Biol 76:1–48.
57. McAlinden A, G Traeger, U Hansen, MA Weis, S Ravindran, L Wirthlin, DR Eyre and R Fernandes. (2013). Molecular properties and fibril ultrastructure of types II and XI collagens in cartilage of mice expressing exclusively the α1(IIA) collagen isoform. Matrix Biol pii:S0945-053X(13)00129-7.
58. Prockop DJ and K Kivirikko. (1995). Collagens: molecular biology, diseases, and potentials for therapy. Annu Rev Biochem 64:403–434.
59. Yamanaka S. (2007). Strategies and new developments in the generation of patient-specific pluripotent stem cells. Cell Stem Cell 1:39–49.
60. Svendsen C. (2013). Back to the future: how human induced pluripotent stem cells will transform regenerative medicine. Hum Mol Genet 22:R32–R38.
61. Guilak F, HA Leddy and W Liedtke. (2010). Transient receptor potential vanilloid 4: The sixth sense of the musculoskeletal system? Ann N Y Acad Sci 1192:404–409.
62. Lewis R, S Ravindran, L Wirthlin, G Traeger, RJ Fernandes and A McAlinden. (2012). Disruption of the developmentally-regulated Col2a1 pre-mRNA alternative splicing switch in a transgenic knock-in mouse model. Matrix Biol A31:214–226.
63. Colnot C. (2005). Cellular and molecular interactions regulating skeletogenesis. J Cell Biochem 95:688–697.
64. Kobayashi T, KM Lyons, AP McMahon and H Kronenberg. (2005). BMP signaling stimulates cellular differentiation at multiple steps during cartilage development. Proc Natl Acad Sci U S A 102:18023–18027.
65. Shu B, M Zhang, R Xie, M Wang, H Jin, W Hou, D Tang, SE Harris, Y Mishina, et al. (2011). BMP2, but not BMP4, is crucial for chondrocyte proliferation and maturation during endochondral bone development. J Cell Sci 124: 3428–3440.
66. Suzuki T, T Notomi, D Miyajima, F Mizoguchi, T Hayata, T Nakamoto, R Hanyu, P Kamolratanakul, A Mizuno, et al. (2013). Osteoblastic differentiation enhances expression of TRPV4 that is required for calcium oscillation induced by mechanical force. Bone 54:172–178.
67. O'Conor CJ, TM Griffin, W Liedtke and F Guilak. (2013). Increased susceptibility of Trpv4-deficient mice to obesity and obesity-induced osteoarthritis with very high-fat diet. Ann Rheum Dis 72:300–304.

Address correspondence to:
Dr. Biagio Saitta
Laboratory of Stem Cell and Matrix Biology
Department of Biomedical Sciences
Medical Genetics Institute
Regenerative Medicine Institute
Cedars-Sinai Medical Center
Los Angeles, CA 90048

E-mail: biagio.saitta@cshs.org

Received for publication January 7, 2014
Accepted after revision February 21, 2014
Prepublished on Liebert Instant Online February 21, 2014